Journal of Experimental Microbiology and Immunology (JEMI) Vol. 18: 102 – 107

Construction of pANPT, a Novel pBR322-derived Plasmid with Deletion of the Tetracycline Resistance Gene

Al-Hassan Al-Shaibani, Dashaylan Naidoo, Kathy Pan, Michelle Tran
Department Microbiology & Immunology, University of British Columbia

Previous studies have shown that despite belonging to the same family of ColE1-type plasmids, the pUC19 plasmid is selectively maintained after a few generations when co-transformed with the pBR322 plasmids into *Escherichia coli* DH5α host cells. Some intrinsic differences between the pUC19 and pBR322 plasmids were proposed as potential explanations, including the size difference of 1675 base pairs between the two plasmids. In this study, we initiated an investigation of the role of plasmid size on the exclusion effect by creating a pBR322 plasmid mutant through the deletion of the tetracycline resistance gene. Inverse PCR with primers designed to specifically direct outwards from the tetracycline resistance gene was employed, creating a product that was ligated to generate this 3173 bp deletion mutant. The identity of the construct created was then confirmed through diagnostic and physiological tests. Even though the calculated size did not precisely match the expected size, relative size comparison as well as the inhibition of growth on tetracycline supplemented media supported the construct identity as a tetracycline gene deletion mutant, named pANPT. This pBR322-derived novel plasmid with size comparable to that of the pUC19 plasmid can be used to explore the role of size on the exclusion effect during the co-transformation of the pUC19 and pBR322 plasmids.

Experimental evidence has shown that despite belonging to the same family of ColE1-type plasmids, the pUC19 plasmid is selectively maintained after a few generations when co-transformed with the pBR322 plasmid into *Escherichia coli* DH5α host cells (1). Three intrinsic differences between the pUC19 and pBR322 plasmids were proposed as potential explanations for pBR322 exclusion: the presence of a *rop* gene in the pBR322 plasmid, the existence of a point mutation in the RNA II gene of the pUC19 plasmid, and the 1675 base pairs size difference between the two plasmids. Previous studies have investigated the differences of *rop* gene and the RNA II point mutation, in both the exclusion effect during co-transformations and copy number of the pBR322 and pUC19 plasmids (1, 2, 3 and 4). The impact of size on determining the preferentially selected plasmid during co-transformations has not been explored extensively - the role of size has only been examined through a comparison between individual transformation efficiencies of the pUC19 and pBR322 plasmids (5, 6).

Maintenance and replication of multiple different plasmids causes metabolic stress on host cells and may increase plasmid instability (6, 7). Therefore, *E. coli* DH5α cells are more likely to preferentially maintain one plasmid and exclude others. Individual transformation studies suggest that the pUC19 plasmid has higher transformation efficiency than the pBR322 plasmid where the transformation efficiency is inversely correlated to plasmid size (5, 6). One explanation for this difference is that when transformed individually, the larger plasmid pBR322 takes longer to replicate and thus results in a lower copy number over time, compared to the shorter the pUC19 plasmid (2). The pUC19 plasmid has an approximate copy number of 60 per cell, whereas the pBR322 plasmid showed a copy number of 20 per cell (1). Preferential maintenance will occur between the pUC19 and pBR322 plasmids, because it is metabolically inefficient to keep two different plasmids that contain the same antibiotic selective marker, the ampicillin resistance gene. Since pUC19 plasmid will theoretically outcompete the pBR322 plasmid in copy number after several generations, the pUC19 plasmid will be more likely to be maintained in *E. coli* DH5α.

In this study, we initiated an investigation on the role of plasmid size on the preferential plasmid maintenance by creating pANPT, a pBR322 plasmid mutant derived by deleting the tetracycline resistance gene. Two previous attempts were made to create deletion mutants of the pBR322 plasmid that would match the size of the pUC19 plasmid through the method of gel extraction (4, 6). However, since gel extraction often results in the excessive loss of the desired DNA fragment, our study took a different approach by using specifically designed primers that face outward from the tetracycline resistance gene and ligating the PCR product to generate pANPT. The removal of the 1194 bp tetracycline resistance gene from the pBR322 plasmid would yield a construct with a similar size of 3173 bp to the pUC19 plasmid (2686 bp). We hypothesized that size is a factor in plasmid maintenance in co-transformations with *E. coli* DH5α cells, and therefore will result in an equal copy number of pUC19 plasmid and the pANPT construct within the cells.

MATERIALS AND METHODS

Bacterial Strains. *Escherichia coli* DH5α with the pBR322 plasmid and *E. coli* DH5α with the pUC19 plasmid were obtained from MICB 421 culture collection of the Microbiology and Immunology Department at the University of British Columbia.

Isolation of plasmid. *E. coli* DH5α with the pBR322 plasmid and *E. coli* DH5α with the pUC19 plasmid were grown in two 4 ml Luria Broth (LB) with 100 µg/ml ampicillin (1) at 37°C, 180 rpm on a shaking platform. Both pBR322 and pUC19 plasmids were isolated using the Fermentas GeneJET Plasmid Miniprep kit (cat#K0503) following the manufacturer's protocol. The isolated plasmids were suspended in 100 µl of Elution Buffer (EB) and quantified using a Thermoscientific NanoDrop 2000c

Spectrophotometer. The average yield from the pUC19 plasmid was more than two-folds lower compared to the pBR322 plasmid.

Primer preparation and PCR. Forward and reverse primers were designed to anneal to the pBR322 plasmid to amplify away from the 86-1276 base pair region (Fig. 1) and eliminate the interrupting tetracycline resistance gene. Primers consisted of complementary sequence to the pBR322 plasmid with the addition of an XbaI site. Forward primer sequence: 5' ACTGCA**TCTAGA**ACACGGTGCCTGACTGCGTT 3'. Reverse primer sequence: 5' CGTCTT**TCTAGA**ATGGAAGCCGGCGGCACCTC 3'. The XbaI sequence is shown in bold. The primers were obtained from Integrated DNA Technologies, and rehydrated to make 100 mM stock solutions. Further dilutions were carried out from the stock solutions to make 10 mM primer solutions, which were then used in PCR reactions. PCR mixtures were made following the Fermentas protocol: 1X Fermentas Pfu buffer with $MgCl_2$ added (supplied with Pfu Polymerase), 10 µM of forward primer, 10 µM of reverse primer, 10 mM dNTPs, 80 ng of the pBR322 plasmid template DNA, and 2.5 U of Fermentas Pfu DNA polymerase (recombinant) (cat#EP0501) with the addition of water to a final volume of 50 µl. Thermocycler parameters were set-up according to the Fermentas protocol (Table 1).

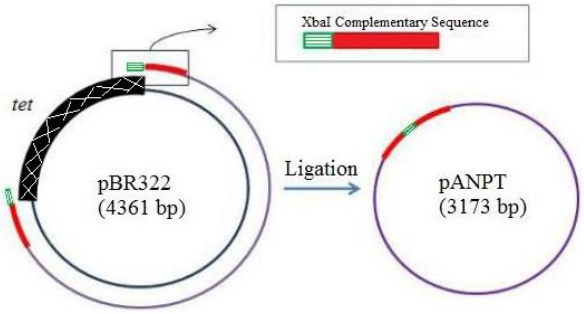

FIG. 1. pBR322 and novel plasmid pANPT**.** A 1194 bp deletion using inverse PCR and addition of the XbaI restriction site.

Gel electrophoresis of PCR products. To confirm the PCR products, 5 µl of each PCR reaction was mixed with 2 µl of Fermentas 6x DNA Loading Dye (cat#R0611). The mixtures were then resolved on 1% (w/v) agarose DNA gel with 1 X TAE Buffer (pH 8.0). 1 µg of Fermentas GeneRuler 1kb DNA Ladder was loaded onto one of the lanes. The gel was run for 50 minutes at 120 V, and stained afterwards in an ethidium bromide bath (0.5 µg/ml) for 15 minutes. The gel was visualized and imaged using an Alpha Imager (Multimage™ Light Cabinet).

Purification of the pBR322 plasmid PCR fragments. PCR products were purified using a Fermentas GeneJET PCR Purification Kit (cat#K0701) following the manufacturer's protocol. The final PCR fragment was eluted in 50 µl EB buffer. DNA concentration was measured using a Thermoscientific NanoDrop 2000c Spectrophotometer.

Restriction digest of the pBR322 plasmid PCR fragments. Sticky ends for ligation were generated by digesting PCR fragments with XbaI (Invitrogen, cat#15226-012), recognition site 5' T/CTAGA 3'. The restriction digest was set-up and performed following the protocol from New England Biolabs (7). The buffer used was 10 X React 2 buffer (Invitrogen, cat#15226-026). The digested pBR322 plasmid PCR fragments were subsequently purified using Fermentas GeneJET PCR Purification Kit (cat#K0701) following the manufacturer's protocol. Final PCR fragment was eluted in 30 µl EB, and measured using a Thermoscientific NanoDrop 2000c Spectrophotometer.

TABLE 1. Thermocycler parameters of the PCR reaction with pBR322 used to generate the pANPT fragment. For optimization purposes, the PCR was conducted with an annealing temperature gradient.

Cycle	Temperature (°C)	Duration of Time (min)
1	95	3
25	95	3
	50,55,57,60,63	1
	72	3.5
1	72	10
	4	15 (hours)

Ligation of the pBR322 plasmid PCR fragment. Compatible sticky ends of the PCR fragment, generated by XbaI restriction digest, were ligated using Fermentas T4 DNA Ligase (cat#EL0011) following a modified version of the manufacturer's protocol: water was added instead of insert DNA. The ligation products were transformed by heat shock into previously prepared chemocompetent *E. coli* DH5α cells, and spread onto LB-ampicillin (LB-Amp) plates (8).

Diagnostic test of candidate pANPT construct. Ten colonies carrying candidate pANPT constructs were selected, and grown overnight in 4 ml LB with 100 µg/mL ampicillin. MP Biomedicals RapidPURE Plasmid Mini kit (cat#2066-400) was used to isolate the plasmids. All ten isolated plasmids were then digested with XbaI restriction endonuclease. Controls of the pBR322 and pUC19 plasmids were linearized with HindIII. All twelve digestions were carried out using a modified version of the protocol from New England Biolabs: 200 ng template DNA, 1 X React 2 buffer (Invitrogen, cat#15226-026), and 1 U of XbaI (Invitrogen, cat#15226-012) or HindIII (Invitrogen, cat#15207-027) with the addition of water to a total volume of 25 µl (9).

Gel electrophoresis for analyzing candidate pANPT construct. Each of the digestion reactions were mixed with 5 µl of Fermentas 6x DNA Loading Dye (cat#R0611), and loaded onto a 1% agarose gel. The gel was run in 1 X TAE buffer for 1.5 hour at 140 V, and post-stained in an ethidium bromide bath (0.5 µg/ml). The gel was visualized and imaged using a UV Gel Doc (Multimage™ Light Cabinet).

Physiological test of candidate pANPT construct. Each *E. coli* DH5α colony containing candidate pANPT construct was streaked onto previously prepared LB-tetracycline plate consisting of 12 µg/ml of tetracycline (EMD-Omnipur, cat#8990) (8). The plates were incubated at room temperature for 3 days, and then observed for growth.

RESULTS

Fragments were generated from the pBR322 plasmid using PCR. The PCR product of the pBR322 plasmid at annealing temperatures between 50 and 60°C gave the same PCR product that appeared to migrate between the size of linearized pUC19 and pBR322 plasmids (data not shown). In order to confirm the fragment sizes and validate the standard curve, the linearized pUC19 and pBR322 plasmid controls were subjected to gel electrophoresis along with three PCR products (Fig. 2). As expected, the PCR fragments generated migrated less than the linearized pBR322 plasmid, but not as far as the pUC19 plasmid, suggesting the PCR fragments are smaller than the pBR322 plasmid and larger than the pUC19 plasmid (Fig.

2). Based on the standard curve calculations the PCR products were 3500 bp, approximately 327 bp more than the expected size of the PCR product (Fig. 3). Linearized pBR322 plasmid was calculated to be 4500 bp, while the linearized pUC19 plasmid was calculated to be 2900 bp (Fig. 3). Similar to the PCR products, both controls were respectively 159 bp and 214 bp larger than their expected sizes. The difference in experimental and expected control sizes gave the Figure 4 standard and all values derived from it a 3.7- 8.0% uncertainty.

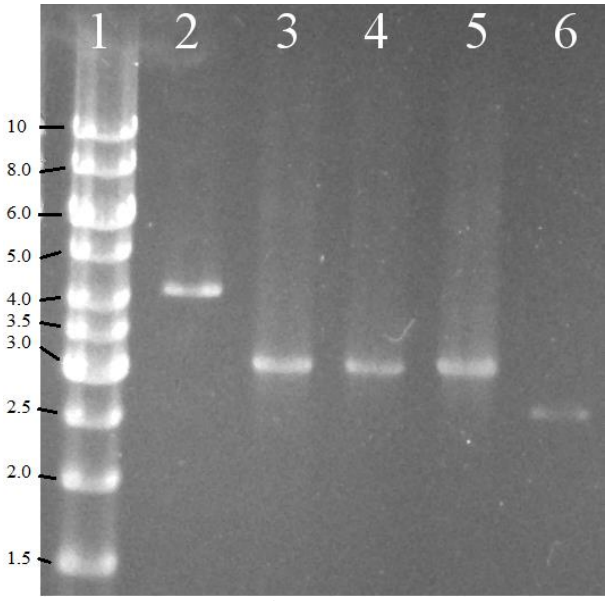

FIG 2. The relative sizes of pANPT PCR constructs prior to transformation compared to linearized pBR322 and pUC19. A GeneRuler 1 kb DNA Ladder in lane 1 was used to determine the sizes of all the bands. Lane 2 contains the pBR322 plasmid digested with HindIII, lanes 3-5 contain the pANPT PCR fragments and lane 6 contains the pUC19 plasmid digested with HindIII.

Calculation of the pANPT plasmid did not precisely match the expected size. The PCR product was ligated and transformed into chemocompetent *E. coli* DH5α cells and spread on both a control LB plate and LB-Amp plate. The 43 colonies on the LB-Amp plate compared to the near confluent lawn on the LB plate suggested that the LB-Amp plate had selected for ampicillin resistant colonies that had been transformed with the ligated PCR product (data not shown). Plasmid DNA was extracted from 10 of the 43 colonies and linearized by restriction endonuclease digestion, then subjected to gel electrophoresis to determine size. Linearized pUC19 and pBR322 plasmids were used as controls to compare the 10 constructs. Nine of the constructs migrated farther than pBR322, but less than pUC19, suggesting the construct sizes to be between the two plasmids (Fig. 4). However, the construct in lane 9 migrated farther than the rest of the candidate constructs and pUC19, indicating a size smaller than the candidate constructs and pUC19 (Fig. 4). A standard curve was generated from Figure 4 to calculate the sizes of the ten constructs and two controls (Fig. 5). The accuracy of the standard curve was validated through the known sizes of pUC19 and pBR322. Plasmid pUC19 was calculated to be 2600 bp, which was 86 bp less than the expected 2686 bp, whereas pBR322 was determined to be 4300 bp, which was 41 bp less than the expected 4361 bp. The difference in experimental and expected control sizes gave the Figure 5 standard and all values derived from it a 0.9-3.2% uncertainty. Nine of the candidate constructs were calculated to be 2700 bp long, which was 473 bp shorter than the expected size of pANPT (Fig. 5). The odd construct, in lane 9, which migrated farther than the rest, was calculated to be 2100 bp long, which is 1073 bp shorter than the expected size of pANPT. Due to the size difference, no further analysis was conducted on the construct from lane 9.

Absence of growth on LB-tetracycline plates confirmed the deletion of the tetracycline gene in all nine candidate pANPT constructs. Since the generation of pANPT constructs from the pBR322 plasmid involved the deletion of the tetracycline resistance gene, physiological testing using LB-tetracycline agar plates was carried out to confirm the candidate pANPT constructs based on their tetracycline sensitive nature. A positive control was employed using the pBR322 plasmid, which encodes for tetracycline resistance. The pUC19 plasmid, which does not contain the tetracycline resistance gene, was used as a negative control. The *E. coli* DH5α strain containing the pUC19 plasmid showed tetracycline sensitivity as its growth was inhibited on the LB-tetracycline plate, while *E. coli* DH5α strain transformed with the pBR322 plasmid showed resistance via growth on the LB-tetracycline plate (data not shown). This proves the LB-tetracycline plates to be selective only for the resistant colonies. All nine *E. coli* DH5α colonies containing candidate pANPT constructs did not grow on LB-tetracycline plates, indicating the deletion of the tetracycline resistance gene (data not shown).

DISCUSSION

The pUC19 and pBR322 plasmids differ in three aspects: the *rop* gene, the point mutation in RNAII, and plasmid size. Majority of the previous studies focused on the effect of the Rop protein and the RNAII point mutation on the low copy number of the pBR322 plasmid, and its exclusion effect when co-transformed with the pUC19 plasmid. Chao *et al.* demonstrated that during individual transformation, the deletion of *rop* gene and the introduction of RNAII point mutation rescued the copy number of the pBR322 plasmid to a level that is comparable to the pUC18 plasmid (a pUC19 plasmid derivative with a differently oriented multiple cloning site) (10). However, during co-transformation with the pBR322 plasmid, Toh showed that the inactivation of the *rop* gene had no impact on the plasmid sustainability (11). These contradictory results beg the question of whether another factor is involved in the determination of plasmid sustainability during co-transformation. Size, being the third difference between the two plasmids, has been shown

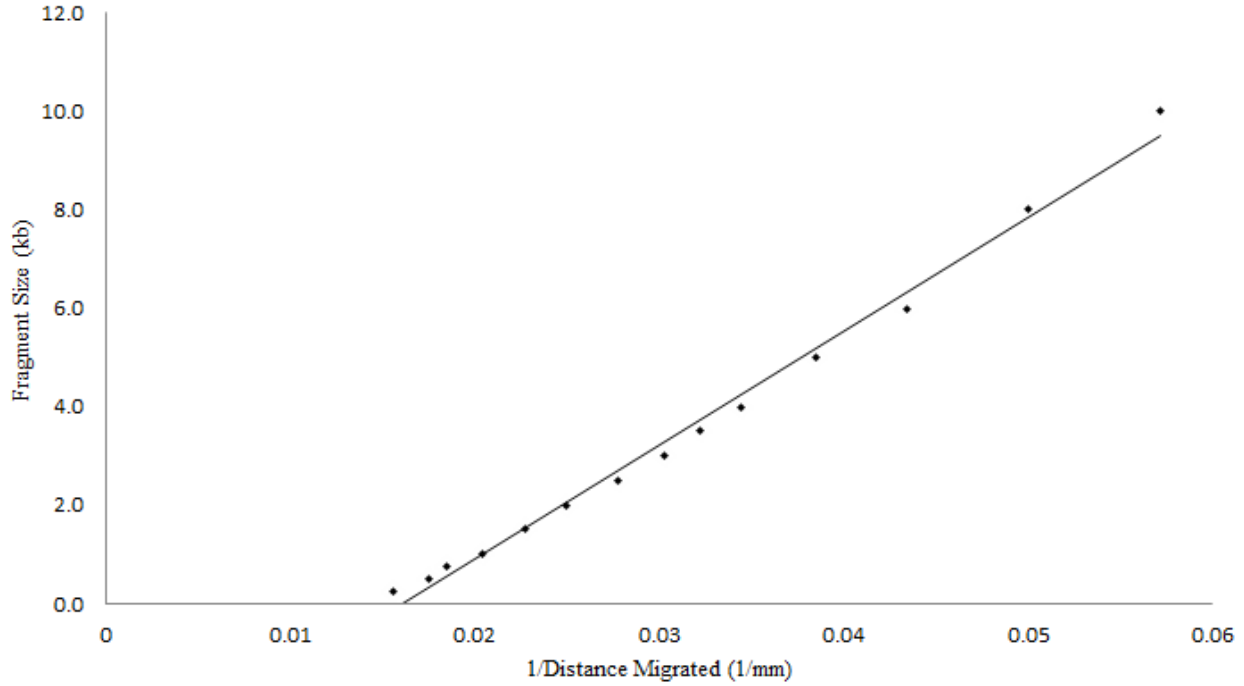

FIG 3. Standard curve generated using GeneRuler 1 kb molecular weight standards (Fig. 2, lane 1). The equation derived from the standard curve is used to calculate the relative sizes of the bands in lane 2-6.

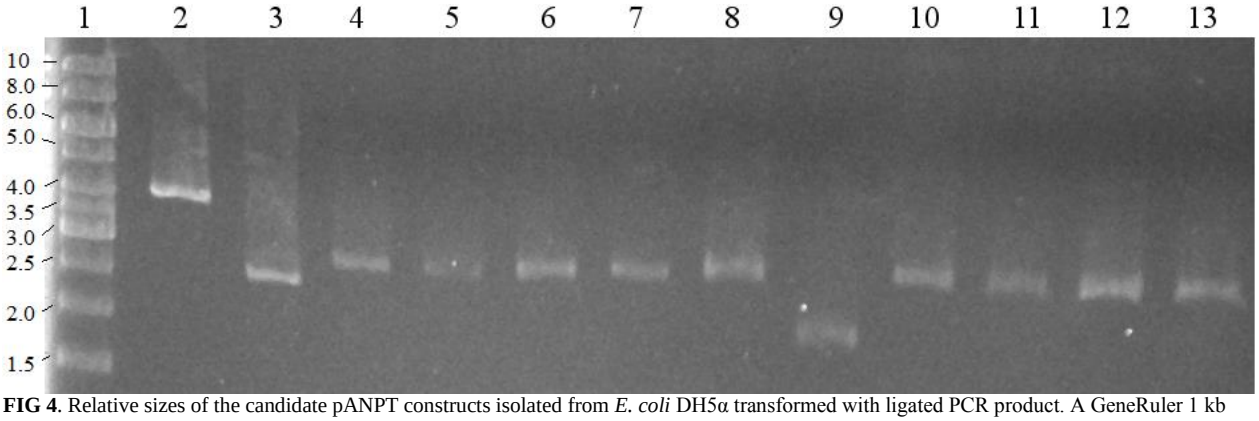

FIG 4. Relative sizes of the candidate pANPT constructs isolated from *E. coli* DH5α transformed with ligated PCR product. A GeneRuler 1 kb DNA Ladder in lane 1 was used to determine the sizes of all the bands. Lane 2 contains the pBR322 plasmid digested with HindIII, lane 3 contains the pUC19 plasmid digested with HindIII and the rest of the lanes contain pANPT from individual clones after digestion with XbaI.

experimentally to inversely affect the transformation efficiency, but was not extensively investigated in the settings of a co-transformation (5). To study the effect of size on the plasmid exclusion effect, the size of either the pBR322 or pUC19 plasmids must be manipulated through the deletion or insertion of a fragment.

Two previous studies attempted to create deletion mutants of the pBR322 plasmid (4, 12). A successful attempt by Glascock resulted in the creation of a pBR322 plasmid deletion mutant with the size of 4275 bp, 86 bp less than the pBR322 plasmid (12). However, this deletion mutant was still 1589 bp longer, and thus 60% larger, than the pUC19 plasmid. On the other hand, our pANPT construct was only 18% larger than the pUC19 plasmid, differing by only 487 bp. As a result, the pANPT construct is more similar in size to the pUC19 plasmid, thus making it a better candidate to use in future co-transformation tests and other exclusion effect studies.

All the candidate constructs, except for one, showed the same pattern when digested in the diagnostic test, suggesting that their identities were the same (Fig.4). The odd construct that migrated farther than the rest can be accounted by a potential slippage in the XbaI site (Fig. 4). Pfu polymerase has an error rate of 1.6×10^{-6}, which translates to one mutation every 625,000 bp (13). Although the error rate is quite minute, it is still possible for mutations in the form of either additions,

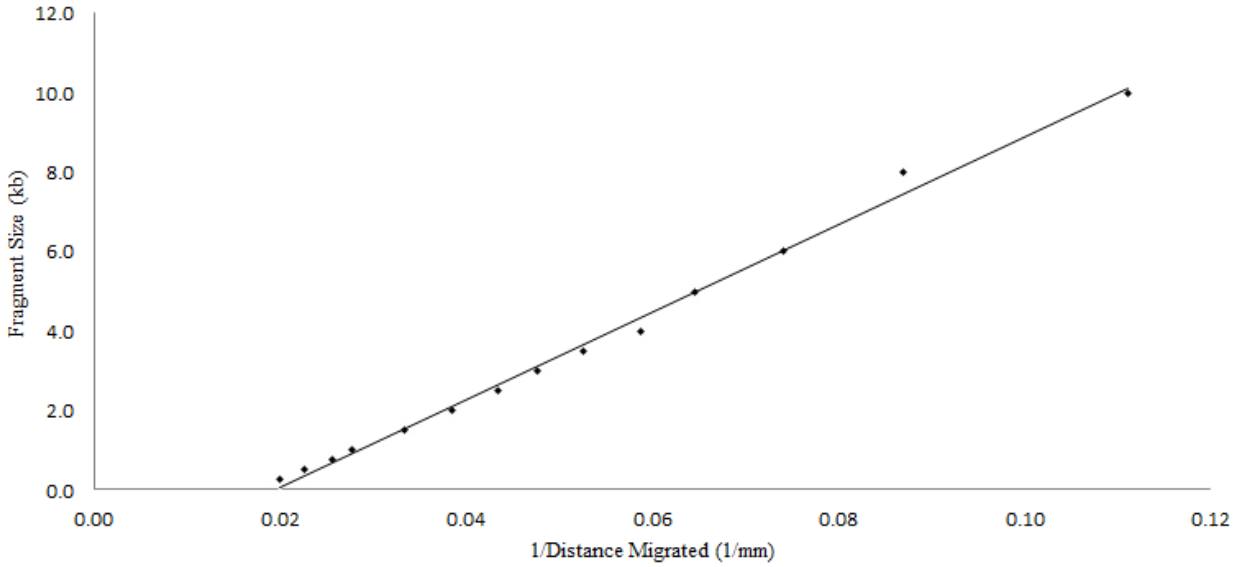

FIG 5. **Standard curve generated using GeneRuler 1 kb molecular weight standards (Fig. 4, lane 1).** The equation derived from the standard curve is used to calculate the relative sizes of the bands in lane 2-13.

deletions or substitutions of a nucleotide to occur. In particular, slippage might have occurred at the end and beginning of PCR amplification, because the polymerase was not bound on either side by base pairs, increasing the likelihood of mutations in the XbaI site (14). Restriction enzymes are highly specific and thus, it is possible that the odd construct obtained a base pair mutation within the XbaI site, and was not linearized. Rather, it remained in its supercoiled form, which is known to migrate farther than linearized DNA (15). Therefore, we eliminated this odd construct as a potential candidate of pANPT.

The diagnostic and the physiological tests of the other nine candidate constructs generally supported the identity of the pANPT construct. The physiological test clearly depicted the absence of the tetracycline resistance gene through the sensitivity of the colonies. In addition, the diagnostic test yielded relative sizes of the pUC19 plasmid, pBR322 plasmid, and pANPT construct, which were consistent with the expected. On the other hand, the calculated sizes determined through the standard curves generated were smaller than the expected by approximately 16% (Fig. 4, 5). Despite taking into account the 0.9 – 3.2% uncertainty calculated from the standard curve using controls of pBR322 and pUC19 plasmids, the constructs are still suggested to be out of the range of the desired size of pANPT (Fig. 5). Additionally, previous analysis of the PCR fragments showed the sizes as being over 3 kbp, within the range of 3.5 - 3.6 kbp long (Fig. 2, 3). Similar to the diagnostic test, the results from the PCR gel were consistent in terms of the relative size of pANPT, but its calculated size did not match precisely with the expected size. The calculated sizes of the PCR fragments were approximately 9% larger than the predicted size of pANPT fragment, which falls out of the range of 3.7 - 8.0% uncertainty calculated based on the controls of the linearized pBR322 and pUC19 plasmids (Fig. 2, 3).

Although both the diagnostic test and the PCR fragments analysis suggest that the constructed plasmid might be smaller than the desired, its potential usefulness in testing the role of size in the exclusion effect would not be affected since the complete ampicillin resistance gene and the *rop* gene are still present. The ampicillin resistance gene, that is the entire constructed plasmid with the tetracycline resistance gene deletion, was maintained as the constructs were all isolated from colonies grown on media selectable for ampicillin resistance. Similarly, the *rop* gene on the constructed plasmid is expected to be unaffected as well. The terminus of the tetracycline resistance gene is 700 bp away from the beginning of the *rop* gene, which is farther than the approximate 500 bp potential over-deletion in the construct generated. Therefore, the possibility of the deletion interfering with the *rop* gene is eliminated.

Based on the results, the pANPT construct, a pBR322-derived plasmid with a deletion of the tetracycline gene was created. The *E. coli* DH5α cells had maintained a plasmid construct with an ampicillin resistance gene, but lacking a tetracycline resistance gene. The relative migration distance, which is farther than linearized pBR322 plasmid and less than the linearized pUC19 plasmid, is indicative of a deletion within the pBR322 plasmid. Although the calculated size of the pANPT construct is not within the range of uncertainty of the expected size for the desired plasmid,

the potential use of the plasmid in the investigation of the role of size in the exclusion effect is unaffected, as both the ampicillin gene and *rop* gene are unaltered.

FUTURE DIRECTIONS

To investigate the effects of plasmid size in the exclusion effect between the pBR322 and pUC19 plasmids, co-transformation tests of the pBR322 plasmid with the pUC19 plasmid, the pBR322 plasmid with the pANPT construct, and the pUC19 plasmid with the pANPT construct should be carried out. This will determine the ability of different but equal-sized plasmids to be retained and co-exist in *E. coli* DH5α cells.

If the decreased size of the pANPT construct can destabilize pBR322 and persist in the presence of pUC19, then a converse construct should be made by adding a 1653 firefly luciferase (FLuc) gene to pUC19 to make construct that is similar in size to pBR322. The pANPT construct and the pUC19 with Fluc insert can both be subjected to co-transformation tests, and further elucidate the role of size in maintenance and coexistence of plasmids within *E. coli* DH5α cells.

ACKNOWLEDGEMENTS

We thank the Department of Microbiology and Immunology of the University of British Columbia for funding the research. We thank Dr. William Ramey for his knowledgeable advice, continuous support and wise guidance. We also thank Kirsten Brown for her advice and support. Furthermore, we would like to extend our gratitude for the other MICB 447 teams including 1ß for chemocompetent *E. coli* DH5α cells, 1∂ for 10x TAE buffer, and 1ζ for tetracycline plates. Finally, we are grateful for the assistance of the Media Room staff.

REFERENCES

1. **Tsui E.** 2006. Determination of exclusion effects of potentially *rop* deficient mutant pBR322 during co-transformation with wild-type plasmid. J. Exp. Microbiol. Immunol. **10**:23-26.
2. **Airo A, Changizi F, Kim M, Wibowo J**. 2011. Construction of pCAWK, a novel pBR322-derived plasmid with insertional inactivation of the *rop* gene. J. Exp. Microbiol. Immunol. **16**:129–135.
3. **Wong J.** 2003. The constructions of pBR322Δ*rop* and its interaction with pUC19 with respect to plasmid copy number and the exclusion effect. J. Exp. Microbiol. Immunol. **4**:55-59.
4. **Heine H.** 2003. Attempts at cloning pBR322Δ(1.1*rop*). J. Exp. Microbiol. Immunol. **4**:42-50.
5. **Szostková M, Horáková D.** 1998. The effect of plasmid DNA sizes and other factors on electrotransformation of *Escherichia coli* JM109. Bioelectroch. Bioener. **47**:319-323.
6. **Chan V, Dreolini LF, Flintoff KA, Lloyd SJ, Mattenley AA.** 2002. The effect of increasing plasmid size on transformation efficiency in *Escherichia coli*. J. Exp. Microbiol. Immunol. **2**:207-223.
7. **Schmidt CM, Shis DL, Nguyen-Huu TD, Bennet MR.** 2012. Stable maintenance of multiple plasmids in *E. coli* using a single selective marker. ACS Synth. Biol. **1:**445-450.
8. **Ausubel FM, Brent R, Kingston R, Moor D, Seidman JG, Smith JA, Struhl K.** 2002. Short protocols in molecular biology, 5th ed. Wiley and Sons.
9. **New England Biolabs**. 2013. Optimizing restriction endonuclease reactions. 1.0.0.3986.
10. **Lin-Chao S, Chen WT, Wong TT.** 1992. High copy number of the pUC plasmid results from Rom/Rop-suppressible point mutation in RNA II. Mol. Microbiol. **22**:3385-93.
11. **Toh SY.** 2013. The study of exclusion effect of pBR322 using its *rop*-inactivated mutant, during co-transformation with pBR322 and pUC19: plasmid copy number does not relate to the exclusion of pBR322. J. Exp. Microbiol. Immunol. **17**:109-114.
12. **Glascock C.** 2003. Effect of altered plasmid size on pBR322 exclusion from pUC19/pBR322 co-transformants. J. Exp. Microbiol. Immunol. **4**:39-41.
13. **Lundberg KS, Shoemaker DD, Adams MW, Short JM, Sorge JA, Mathur EJ.** 1991. High-fidelity amplification using a thermostable DNA polymerase isolated from *Pyrococcus furiosus*. Gene. **1**:1-6.
14. **Eckert KA, Kunkel TA**. 1991. DNA polymerase fidelity and the polymerase chain reaction. Genome Res. **1:**17-24.
15. **Nicholson WL, Setlow P.** 1990. Dramatic increase in negative superhelicity of plasmid DNA in the forespore compartment of sporulating cells of *Bacillus subtilis*. J. Bacteriol. **172**:7-14.